Molecular switches controlled by light

Devens Gust, Thomas A. Moore and Ana L. Moore

The photochemical processes of singlet–singlet energy transfer and photoinduced electron transfer are important not only in natural and artificial photosynthetic energy conversion, but also in a variety of other scientific and technological applications. Controlling these functions at the molecular level using outside stimuli is an interesting scientific challenge. Photochromes, organic molecules that are isomerized by light between two stable forms, can be covalently linked to other chromophores, and changes in their properties resulting from photoisomerization used to switch electron and energy transfer on or off. Simple single- and double-throw molecular switches have been constructed, as well as Boolean logic gates. Such molecules are potentially useful in light-controlled molecular data processing and storage applications.

Introduction

The heart of a digital electronic computer is a group of switches that communicate *via* electrons flowing among them. By analogy, a binary computer based on molecules would require an ensemble of molecular switches that could communicate with one another. Of the various ways in which

Department of Chemistry and Biochemistry, Arizona State University, Tempe, AZ 85287-1604, USA. E-mail: gust@asu.edu; Fax: 1-480-965-2747; Tel: 1-480-965-4547

Devens Gust is Foundation Professor of Chemistry and Biochemistry at Arizona State University. His main scientific interests are in the areas of organic photochemistry, molecular logic, and artificial photosynthesis. He received his BS degree in Chemistry from Stanford University, and his PhD at Princeton University, and was a postdoctoral associate at Caltech before joining ASU. He received the Inter-American Photochemical Society Award in Photochemistry in 2005, and serves on the editorial boards of Nanotechnology and the Journal of Porphyrins and Phthalocyanines.

Thomas A. Moore is Professor of Chemistry and Biochemistry at Arizona State University. After receiving the BA and PhD degrees in Biochemistry from Texas Tech University, he spent three years as a postdoctoral associate at the University of Washington. In 1976, he joined Arizona State University. He received the Senior Research Award from the American Society for Photobiology in 2001 and served as President of the Society in 2003. He is on the editorial boards of the Journal of Photoscience and Carotenoids.

Ana L. Moore is Professor of Chemistry and Biochemistry at Arizona State University. She received the Bachelor of Pharmacy degree at the Universidad Nacional de La Plata, Argentina, and the MS in Chemistry from the Universidade Federal do Rio de Janeiro, Brazil, before coming to Texas Tech University, where she was awarded the PhD in Chemistry. After spending three years as a postdoctoral associate at the University of Washington, she moved to Arizona State University. She serves on the editorial advisory board of Accounts of Chemical Research.
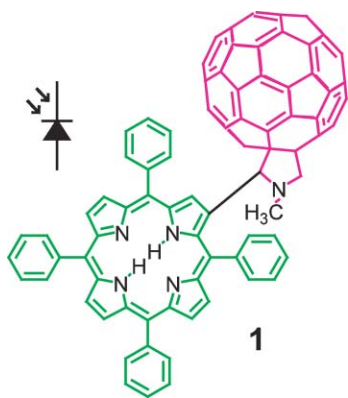
molecules can exchange information with one another and their environment, two of the most appealing from the computational point of view are electronic and photonic interactions. Neither of these requires physical access to a particular molecular switch for addition of chemicals, or translational motion of molecules. In principle, electronic communication would permit interfacing molecular logic with conventional electronic devices. Photonic communication would allow interfacing using light, which can be precisely controlled in the energy and time domains, can pass through materials, and can be spatially controlled in three dimensions.

Molecules can readily communicate using these media. Electronic excitation energy may be transferred by singlet–singlet or triplet–triplet energy transfer processes. Electron transfer can be initiated by ground state or excited state processes. Indeed, such processes lie at the heart of photosynthetic solar energy conversion. Porphyrin (P) fullerene (C_{60}) dyad **1** (Fig. 1) illustrates communication between chromophores within the same molecule by both electronic and photonic means.[1]

Porphyrins such as that in **1** absorb light at many wavelengths in the visible region, including a Soret absorption band at 427 nm and four weaker Q-bands at 519, 555, 595 and 653 nm. The lifetime of the porphyrin first excited singlet state of model porphyrins in a solvent such as benzonitrile is 9.6 ns. Decay pathways are intersystem crossing to the triplet state, internal conversion to the ground state, and fluorescence. Spectroscopic investigations reveal that excitation of **1** with light at 590 nm generates the porphyrin first excited singlet state $^{1}P–C_{60}$. The linkage of the fullerene to the porphyrin enables two additional pathways for excited state decay. One is photoinduced electron transfer to the fullerene to generate the $P^{\bullet+}–C_{60}^{\bullet-}$ charge-separated state (time constant τ = 5.6 ps). The second is singlet–singlet energy transfer to the fullerene, yielding the fullerene first excited singlet state $P–^{1}C_{60}$ (τ = 14 ps). Because these two interchromophoric processes occur much more rapidly than the usual photophysical decay paths mentioned above, they dominate the decay process in the dyad. The fullerene first excited singlet state lifetime in model

Fig. 1

fullerenes is 1.36 ns. In dyad **1**, it is shortened to 74 ps by photoinduced electron transfer from the porphyrin, also producing $P^{\bullet+}$–$C_{60}{}^{\bullet-}$. *Via* the two pathways, the charge-separated state forms with a quantum yield Φ of 99%. It preserves about 1.58 eV of the excitation energy as electrochemical potential and has a lifetime of 290 ps, decaying back to the ground state. Thus, **1** acts as a kind of molecular photovoltaic.

Although dyad **1** demonstrates two modes of interchromophore communication, it does not provide a mechanism for switching electron or energy transfer on and off. How might one design molecular switches to control these processes, and thus provide at least a conceptual basis for molecular computation? We have been investigating the use of photochromes for this purpose. Photochromic molecules exist in two stable isomeric forms that can be interconverted using light of appropriate wavelengths.[2] In the most useful photochromes, thermal interconversion is slow at ambient temperatures. A variety of molecular switches, some based on photochromes, have been investigated.[3–25]

Of the various ways in which photochromes could be used to control energy and electron transfer between chromophores, donors and acceptors, we have focused on three: switching the electron donor properties of the photochrome, switching the electron acceptor properties of the photochrome, and switching the energies of the excited singlet states of the photochrome. These methods have allowed us to prepare molecule-based, light-operated single and double-throw switches for photoinduced electron transfer and various molecular Boolean logic gates (AND, INHIBIT, XOR, *etc.*). Several of these will be discussed below.

Excited states are highly energetic species with many possible pathways for dissipation of energy. A simple singlet excited state typically decays by three photophysical processes: internal conversion, fluorescence, and intersystem crossing to the triplet manifold. Photochrome excited states also decay by photoisomerization reactions, and sometimes by competing side reactions. In a dyad of two chromophores which can demonstrate energy and electron transfer, there are at least 11 rate constants to be balanced. With a triad of three chromophores, there are more than 24 relevant rate constants. The triplet manifold, or inclusion of a photochrome, introduces additional webs of decay possibilities. Designing a
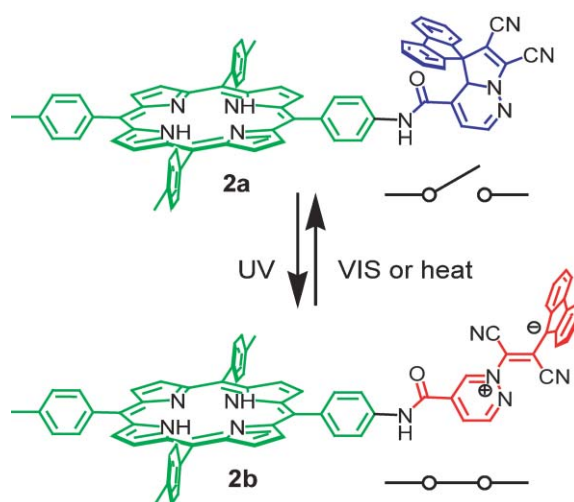

Fig. 2   A molecular single-throw switch. In **2a**, photoinduced electron transfer does not occur. UV irradiation converts **2a** to **2b**, in which the betaine moiety can be reduced by the porphyrin first excited singlet state to yield a charge-separated state. Visible irradiation converts **2b** back into the inactive form.

molecule in order to favor a particular set of events requires sensitive control of all of these rate constants, and is a severe test of our understanding of the factors that influence photophysical and photochemical processes.

Single-throw switches

The simplest kind of switch is a single-throw switch, which has two states: *on* and *off*. Dyad **2** (Fig. 2) illustrates such a molecular switch.[26] It consists of a tetraarylporphyrin linked to a photochrome related to the dihydroindolizines.[27,28] The photochromic moiety of **2** exists in two isomeric forms. The spirocyclic DHI form, shown in **2a**, does not absorb light in the visible region (see spectrum in Fig. 3), and has a relatively low reduction potential of −1.18 V *vs.* SCE. Irradiation with UV light (*e.g.* 366 nm) leads to photoisomerization of **2a** to **2b**, in which the photochrome has a betaine structure (BT) and absorbs strongly in the 550-nm spectral region. The reduction potential of the betaine moiety is −0.7 V, making it a good electron acceptor. Visible light (>590 nm) or heat convert **2b**
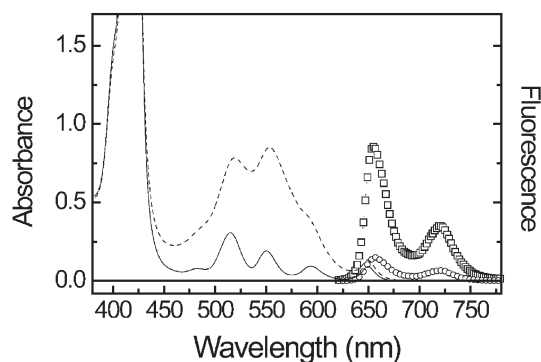

Fig. 3   Absorption (—) and fluorescence (□) spectra of P–DHI dyad **2a**, and corresponding absorption (---) and emission (○) spectra of P–BT dyad **2b**, in 2-methyltetrahydrofuran.

back into **2a**. Excitation of **2a** at 575 nm with a laser pulse yields the porphyrin first excited singlet state [1]P–DHI, which then decays to the ground state in 11.5 ns. This is a typical excited state lifetime for a porphyrin of this type, which decays by intersystem crossing, internal conversion and fluorescence. The DHI has no effect on the porphyrin excited state.

When the molecule is photoisomerized to **2b** using UV light, the photochromic moiety becomes a viable electron acceptor. Excitation of the porphyrin at 575 nm again gives the porphyrin first excited singlet state ([1]P–BT), but this state now decays by photoinduced electron transfer to the betaine to produce P$^{\bullet+}$–BT$^{\bullet-}$ with a time constant of 50 ps and a quantum yield of 100%. The charge-separated state rapidly (2.9 ps) decays to the ground state.

Dyad **2** thus acts as a light-controlled molecular switch. When **2** is in the P–DHI form, the switch is open, and photoinduced electron transfer from the porphyrin does not occur. Closing the switch by photoisomerization to **2b** leads to efficient electron transfer and a charge-separated state. The switch may be cycled a number of times (Fig. 4), although some photodecomposition does occur, especially in the presence of oxygen.

Molecular triad **3** (Fig. 5) is an example of an electron transfer switch based on changes in the oxidation potential of a photochrome.[29] The molecule consists of a porphyrin chromophore linked covalently to both a fullerene electron acceptor and a dihydropyrene[30–32] photochrome. In the design of the molecule, the electronic interactions between the photochrome and porphyrin have been adjusted so that the dihydropyrene photoisomerization still occurs in spite of the attached porphyrin and potentially competing energy or electron transfer processes. In structure **3a**, the photochrome is in the cyclophanediene form, which absorbs light only in the ultraviolet. Excitation of the porphyrin moiety of a 2-methyl-tetrahydrofuran solution of **3a** yields CPD–[1]P–C$_{60}$, which decays by photoinduced electron transfer to the fullerene (as in dyad **1**) to yield a CPD–P$^{\bullet+}$–C$_{60}^{\bullet-}$ charge-separated state (τ = 36 ps). This rapid charge separation occurs because there is substantial thermodynamic driving force for photoinduced electron transfer. The porphyrin first excited singlet state lies 1.91 eV above the ground state, whereas CPD–P$^{\bullet+}$–C$_{60}^{\bullet-}$ is at 1.58 eV, as estimated from the redox potentials of model
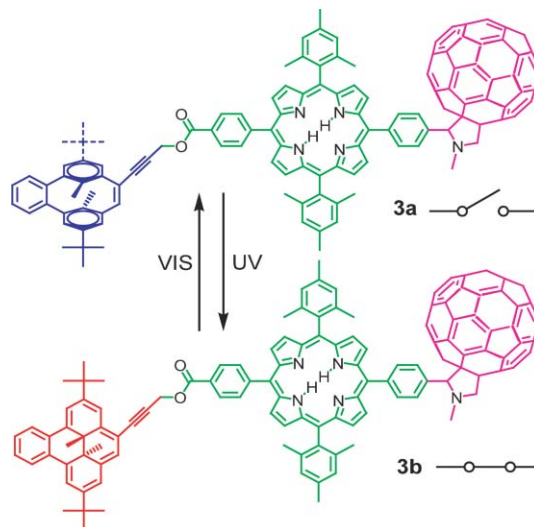
Fig. 5 CPD–P–C$_{60}$ molecular triad **3a** is converted to the dihydropyrene isomer **3b** (DHP–P–C$_{60}$) upon irradiation with UV light, and visible irradiation regenerates **3a**. The triad acts as a single-throw molecular switch based on the changes in the oxidation potential of the photochrome.

compounds. The charge-separated state forms with a quantum yield of unity, but decays rapidly to the ground state with a time constant of 3.3 ns.

Irradiation of **3a** with UV light at 254 nm converts the molecule to **3b**, in which the photochrome is in the dihydropyrene form. The dihydropyrene absorbs in the visible region (450–550 nm), and can be isomerized back to the cyclophanediene by visible light. The photochemistry of **3b** is quite different from that of **3a**. Time-resolved spectroscopic studies show that excitation of the porphyrin of **3b** generates DHP–[1]P–C$_{60}$, which decays mainly by photoinduced electron transfer to the fullerene, giving DHP–P$^{\bullet+}$–C$_{60}^{\bullet-}$. However, before the charge-separated state can recombine to the ground state, an electron migrates from the DHP moiety to the porphyrin, producing DHP$^{\bullet+}$–P–C$_{60}^{\bullet-}$. This charge shift reaction occurs because the dihydropyrene is a much better electron donor than the CPD moiety (and the porphyrin). The DHP$^{\bullet+}$–P–C$_{60}^{\bullet-}$ state lies only 1.16 eV above the ground state, and the thermodynamic driving force for the charge shift is a healthy 0.42 eV. The overall yield of the final charge-separated state, based on light absorbed, is 94%.

The DHP$^{\bullet+}$–P–C$_{60}^{\bullet-}$ state has a long lifetime for charge separation, 2.0 μs. The reason for the great increase in lifetime over that of CPD–P$^{\bullet+}$–C$_{60}^{\bullet-}$ is that the charges in DHP$^{\bullet+}$–P–C$_{60}^{\bullet-}$ are much farther apart, and the reduced electronic coupling interaction slows the rate of electron transfer. A similar strategy is used in photosynthesis to retard charge recombination, and the same approach has been used to prepare artificial photosynthetic reaction centers with long-lived, energetic charge-separated states.[33–35] The occurrence of charge separation in **3** and the lifetime of the charge-separated state may be conveniently monitored by measuring the transient absorbance of the fullerene radical anion at 1000 nm, as shown in Fig. 6. The time resolution of the spectrometer used to obtain these data was such that although
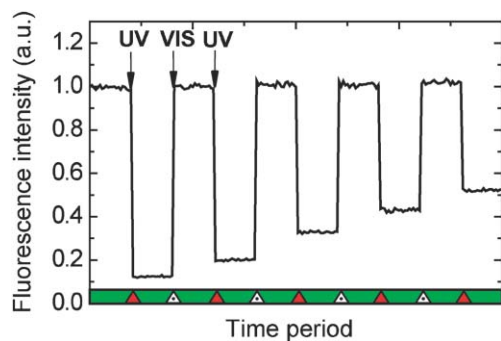

Fig. 4 Photochemical cycling of dyad **2** as detected by monitoring porphyrin fluorescence at 720 nm. Green bar: fluorescence measurement for 12 s, red triangles: UV irradiation for 60 s at 366 nm, white triangles: visible irradiation for 3600 s.
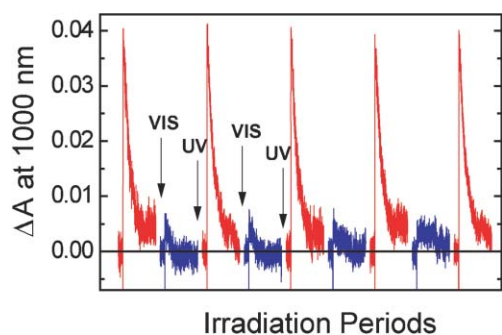
Fig. 6 Operation of molecular single-throw switch **3** in 2-methyltetrahydrofuran solution. Initially (at left), the molecule is in the DHP–P–C_{60} form **3b**, and the switch is in the *on* position. Excitation of the porphyrin leads to formation of DHP$^{\bullet+}$–P–$C_{60}{}^{\bullet-}$, and the decay of the absorbance of this charge-separated state at 1000 nm on the ns time scale is shown in red. Visible irradiation (arrow) isomerizes the molecule to CPD–P–C_{60} form **3a**, turning the switch *off*. Excitation of the porphyrin in **3a** does not produce a long-lived charge-separated state, and no significant transient absorption is observed (blue data). The figure shows performance over several *on–off* cycles.

the DHP$^{\bullet+}$–P–$C_{60}{}^{\bullet-}$ state could be readily detected, the short-lived CPD–P$^{\bullet+}$–$C_{60}{}^{\bullet-}$ decays before the first datum is obtained.

Molecule **3** functions as a single-pole molecular switch. The "readout" of the switch is the long-lived charge separation in the DHP$^{\bullet+}$–P–$C_{60}{}^{\bullet-}$ state. This can be detected spectroscopically at 1000 nm, as described above. In principle, it could also be detected electrically if "wires" could be attached to the fullerene and DHP moieties in order to include such molecules in an electrical circuit. When **3** is in the CPD form, excitation of the porphyrin moiety does not lead to long-lived charge separation, and the switch is *off*. UV light "throws" the switch to the DHP–P–C_{60} form, which does display long-lived charge separation when the porphyrin is excited (switch is turned *on*). Visible light isomerizes the molecule back to CPD–P–C_{60}, turning the switch *off* once again. A number of such cycles are illustrated in Fig. 6.

A double-throw switch

A double-throw switch is a two-position switch that directs current through one circuit or a second, depending upon its position. Fig. 7 shows the isomeric forms of triad **4**, which functions in this manner.[36] As illustrated by molecules **1–3**, both C_{60} and the BT chromophore have reduction potentials that make them suitable electron acceptors for porphyrin excited singlet states, but the DHI chromophore is a poor acceptor. Thus, excitation of the porphyrin moiety of **4a** would be expected to lead to photoinduced electron transfer to the fullerene to yield DHI–P$^{\bullet+}$–$C_{60}{}^{\bullet-}$. As illustrated for **2**, irradiation of **4a** with UV light should induce photoisomerization to **4b**. Although **4b** features two electron acceptor moieties, the design goal is that photoinduced electron transfer to BT should occur much more rapidly than transfer to C_{60}, leading to BT$^{\bullet-}$–P$^{\bullet+}$–C_{60}. Thus, photoisomerization of **4a** to **4b** would redirect photoinduced electron transfer down a new pathway, leading to a double-throw switch.
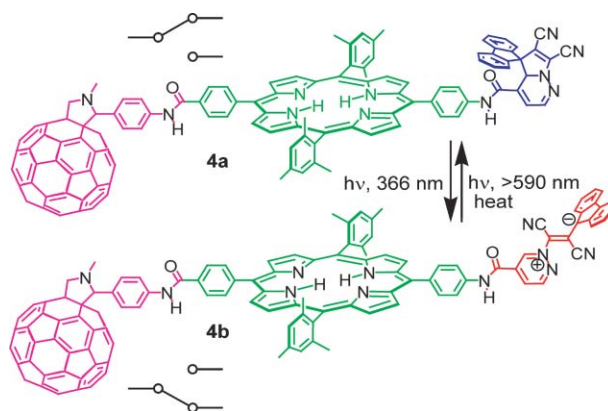

Fig. 7 Light-controlled double-throw switch. In **4a**, excitation of the porphyrin leads to photoinduced electron transfer to produce DHI–P$^{\bullet+}$–$C_{60}{}^{\bullet-}$. Photoisomerization with UV light forms **4b**. Excitation of **4b** results in formation of BT$^{\bullet-}$–P$^{\bullet+}$–C_{60}. Thus, photoinduced electron transfer is directed down one branch of the molecule or the other, depending upon the state of the photochromic switch.

The results discussed above for **2** and **3** demonstrate that the rate constant for electron transfer from the porphyrin moiety of **3** to the fullerene is larger than that for transfer from the porphyrin moiety of **2** to BT. Thus, the corresponding rate constants in **4** have been "tuned" in order to reduce the rate of electron transfer from the porphyrin excited state to the fullerene, relative to **3**. In general, such tuning can be done by altering either the driving force for photoinduced electron transfer or the electronic coupling of the initial and final states, in accord with the Marcus–Hush theory of electron transfer.[37–40] In **4** the desired result was achieved by altering electronic coupling. Electron transfer in such molecules occurs *via* a superexchange mechanism, whereby electronic orbitals of the covalent "bridge" between the donor and acceptor moieties mix with the donor and acceptor orbitals to enhance the electronic coupling. In **4**, the bridge between the porphyrin and the fullerene has been extended, relative to that in **3**, decreasing coupling and therefore the rate constant for photoinduced electron transfer.

Spectroscopic studies of triad **4** in 2-methyltetrahydrofuran solution demonstrate that the molecule functions as desired. Excitation of the porphyrin of DHI–P–C_{60} **4a** is followed by photoinduced electron transfer to the fullerene with a time constant of 2.4 ns, giving DHI–P$^{\bullet+}$–$C_{60}{}^{\bullet-}$ with a quantum yield of 82%. This charge-separated state decays with a lifetime of 4.76 ns. Irradiation of **4a** with UV light at 366 nm converts **4a** to BT-P–C_{60} triad **4b**. Excitation of **4b** is followed by photoinduced electron transfer from the porphyrin to the BT moiety, giving BT$^{\bullet-}$–P$^{\bullet+}$–C_{60} with a time constant of 56 ps and a yield of 99%. The yield of electron transfer down the "wrong" path to produce BT–P$^{\bullet+}$–$C_{60}{}^{\bullet-}$ is only ~1%. Irradiation of **4b** with visible light ($\geqslant$590 nm) converts the triad back to the DHI isomer **4a**.

The function of **4** as a double-throw molecular switch is illustrated by Fig. 8, which also shows photochemical cycling of the triad. The transient absorbance at 1000 nm following laser excitation of the porphyrin at 650 nm is shown. The high transient absorbance values were obtained from the molecule
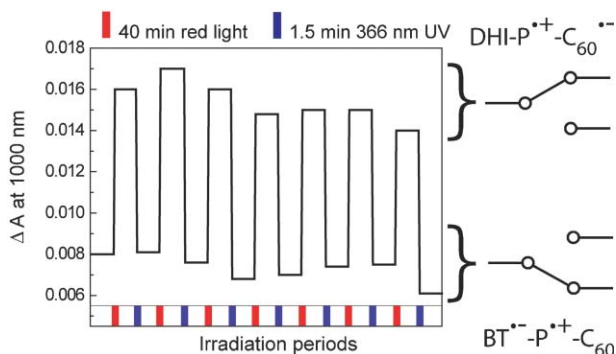
Fig. 8 Cycling of molecular double-throw switch **4**. Irradiation with red light photoisomerizes the molecule to the DHI–P–C_{60} form, in which photoinduced electron transfer occurs from the porphyrin to the fullerene, as indicated by the high transient absorbance values at 1000 nm. UV light converts the molecule to the BT–P–C_{60} form, wherein photoinduced electron transfer occurs preferentially to the betaine, whose radical ion lacks strong absorbance in the 1000 nm region.

in the DHI–P–C_{60} form, and reflect the absorbance of the fullerene radical anion of DHI–$P^{\bullet+}$–$C_{60}^{\bullet-}$. The low transient absorbance values were measured for the sample with the molecule mainly in the BT–P–C_{60} form, and indicate the absence of fullerene radical anion due to preferential formation of $BT^{\bullet-}$–$P^{\bullet+}$–C_{60}. There is little or no photodegradation during this cycling. The variations in ΔA are due mainly to variations in the intensity of the excitation laser.

Molecular logic gates

If simple molecular switches such as those above can be suitably combined, molecular logic gates may be produced. We illustrate this idea with triad **5** (Fig. 9), which comprises a porphyrin linked to both dihydroindolizine and dihydropyrene type photochromes.[41] Key to the design of such molecules is ensuring both the ability to independently photoisomerize the two photochromes in each direction and the ability to independently quench the porphyrin excited singlet state by photoinduced electron transfer or energy transfer. If these requirements are met, the porphyrin moiety can serve to detect and integrate the states of both photochromes and provide a "readout" signal that characterizes the overall state of the molecule.

Triad **5** meets these criteria, and functions as a molecular AND logic gate.[41] The Boolean AND gate has the truth table shown in the first three columns of Table 1. The gate has two inputs, A and B, and an output. Each input may be in either the *on* (1 in Table 1) or *off* (0 in Table 1) state. If both inputs are *off*, the output of the gate is *off*. If either input A or input B is switched *on*, the output remains *off*. However, if *both* inputs are *on*, the output switches to the *on* state. From Fig. 9, it can be seen that molecule **5** can in principle exist in four isomeric forms, **5a–5d**. In the molecular AND gate, each of these forms is associated with one of the logic states listed in Table 1, as shown in the fourth column.

In order to realize the AND gate function with **5**, an experimental protocol for placing the majority of the
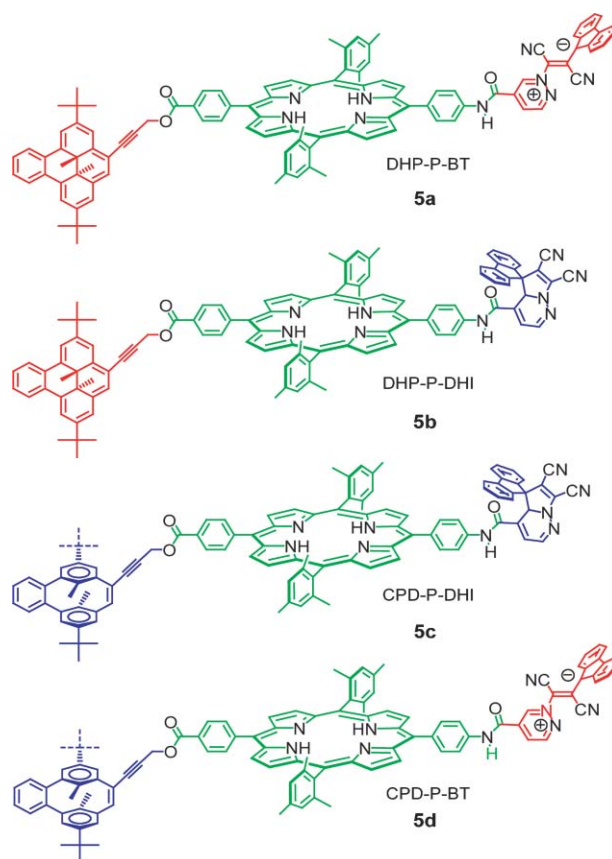

Fig. 9 Four isomeric forms of triad **5**.

molecules in any of the four states by application of combinations of external stimuli must be found. This has been accomplished. Input A is defined as heating for 30 min at 55 °C (or pulsed IR laser irradiation), and input B is red light (590 nm $< \lambda <$ 900 nm) irradiation. The output is strong fluorescence from the porphyrin (*e.g.* at 720 nm).

The molecule, dissolved in 2-methyltetrahydrofuran, is initially set in the state DHP–P–BT. The molecule was converted to this initial state, and reset after each logic operation, by irradiation with light at 366 nm followed by 254 nm light. When the molecule is in this form (**5a**), the BT moiety strongly quenches the porphyrin first excited singlet state by photoinduced electron transfer, as discussed above for dyad **2**. (The time constant for this process is 43 ps, and the unquenched porphyrin singlet excited state lifetime is 11 ns.) The DHP moiety also quenches the porphyrin first excited singlet state (likely also by photoinduced electron transfer[41]), with a time constant of 1.8 ns. Thus, the porphyrin fluorescence of DHP–P–BT is strongly quenched by both of

Table 1 Truth table for AND gate

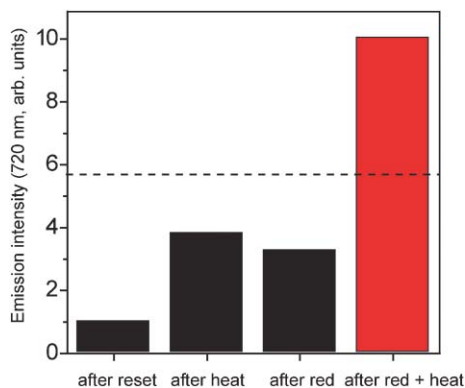| Input A (heat or IR)	Input B (red light)	Output (porphyrin fluorescence)	State of **5**
0	0	0	DHP–P–BT
1	0	0	DHP–P–DHI
0	1	0	CPD–P–BT
1	1	1	CPD–P–DHI

Fig. 10 AND gate function of triad **5**. The bars show the fluorescence intensity after resetting the gate, and following application of the possible combinations of the two inputs. The gate turns *on* only after application of both inputs (red bar), as required for AND gate performance.

the appended photochromes, and only weak emission is observed. The fluorescence output is below a threshold level, and the AND gate output is *off*. If neither input is applied, the gate remains *off*, as thermal isomerization at room temperature is slow (first line of Table 1). If input A is applied, BT is converted to DHI, yielding DHP–P–DHI. The DHI does not quench porphyrin fluorescence, but the DHP is still an active quencher, so the gate output remains *off*. Alternatively, if input B is turned on, DHP is isomerized to CPD, which does not quench fluorescence. But BT is essentially unaffected by the amount of red light employed, and continues to quench porphyrin fluorescence, maintaining the gate in the *off* state. Finally, applying both inputs isomerizes both photochromes, yielding CPD–P–DHI. Neither photochrome quenches the porphyrin excited singlet state, and strong fluorescence is observed, signaling that the output is in the *on* state. Thus, the molecule meets the criteria for an AND gate. The experimental porphyrin emission intensities at 720 nm are shown in Fig. 10.

The operation of the gate through several cycles is illustrated in Fig. 11, wherein the porphyrin emission intensity is indicated following each input. The actual signal-to-noise obtained is evident from these data. Following each
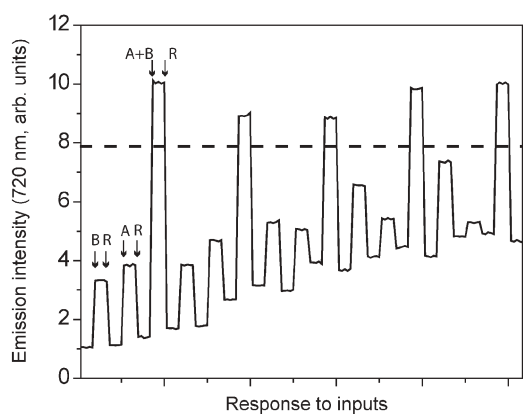

Fig. 11 Cycling of AND gate **5**. The dashed line indicates a threshold level. The gate output is *on* when the amplitude of fluorescence exceeds this level. A: input A applied, B: input B applied, R: reset applied.

measurement, the gate was reset to its initial state and another measurement taken prior to initializing the next input. It is clear that although the gate may be cycled many times while still retaining a sufficient signal-to-noise ratio to allow detection of the state of the output, the emission intensity in the initial state increases following each reset operation. This is due for the most part to photodecomposition of the dihydroindolizine moiety.

During the operation of the gate, the two photochromes serve to record the input history (A *on*, B *on*, *etc.*). The porphyrin correlates the responses of the two photochromes to the inputs, and generates outputs that are representative of the states of both photochromes, as required for the AND gate function. This correlation can occur because the porphyrin excited singlet state communicates electronically with each photochromic switch.

Although the purpose of this research has been to investigate the feasibility of realizing logic functions photochemically in the dyads and triads (and not to demonstrate the practicality of any actual devices), it is interesting to consider the speed of the various switching operations in the AND gate. The readout response time is limited only by the time it takes to detect the porphyrin fluorescence, and is on the ns time scale or less. The time required for isomerization of the photochromes depends, of course, on the light intensity and the temperature or IR laser flux, as appropriate. For example, the slowest real-time step in the switching sequence for **5** above was irradiation with a pulsed IR laser for 3 h. This corresponds to only 540 µs of actual irradiation time. An increased light flux would shorten the time required accordingly. In addition, the experiments were carried out in standard 1 cm cuvettes with sample sizes of ~2 mL. As the gates are of molecular dimensions, and the readout is fluorescence, which may in general be detected even with single-molecule sensitivity, it should be possible to carry out these experiments with very small volumes, and consequently shorter photoisomerization periods.

Triad **5** can also function as a molecular INHIBIT gate by choosing suitable initial conditions and inputs. An INHIBIT gate can be considered as an AND gate with one input inverted by a NOT function. Like the AND gate, the INHIBIT gate (Table 2) has two inputs and an output. When neither input is *on*, the gate is *off*. Switching on input A turns the gate *on*. However, turning on input B does not switch the gate *on*. In addition, switching both inputs *on* leaves the gate in the *off* position. Thus, input B inhibits the gate from responding to input A.

When triad **1** is used as an INHIBIT gate, it is set initially in the state DHP–P–DHI. This was done by exposing the sample dissolved in 2-methyltetrahydrofuran to 366 nm irradiation,

Table 2 Truth table for INHIBIT gate

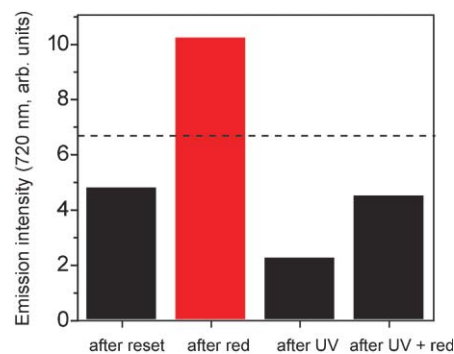| Input A (red light)	Input B (UV light)	Output (porphyrin fluorescence)	State of **5**
0	0	0	DHP–P–DHI
1	0	1	CPD–P–DHI
0	1	0	DHP–P–BT
1	1	0	CPD–P–BT

Fig. 12 INHIBIT gate function of triad **5**. The bars show the fluorescence intensity after resetting the gate, and following application of the possible combinations of the two inputs. The gate turns *on* only after application of input A (red bar), as required for INHIBIT gate performance.

Fig. 13 Isomeric forms of molecular switch **6**.

254 nm irradiation, and finally 55 °C for 30 min. Alternatively, exposure to IR laser pulses could be substituted for the heating step. In the initial, DHP–P–DHI, state, the porphyrin fluorescence, which comprises the output of the gate, is quenched by DHP and the gate is *off*. Input A is red light which isomerizes DHP, leading to CPD–P–DHI. Porphyrin fluorescence is not quenched in this state, and the gate is turned *on*. Input B is UV irradiation at 366 nm. This converts DHP–P–DHI to DHP–P–BT, wherein the porphyrin excited state is quenched by both photochromes, porphyrin emission is weak, and the gate remains *off*. Finally, irradiation with both red light and 366 nm light (both inputs on) isomerizes both DHI and DHP, generating CPD–P–BT. In this isomer, the porphyrin fluorescence is quenched by BT, and the gate output is *off*. Between applications of the various inputs, the gate is reset to its initial condition as discussed above. Thus, the requirements for an INHIBIT gate are met.

Fig. 12 shows the measured relative fluorescence emission intensities for a typical sample in the initial state and following the various combinations of inputs. Clearly, it is easy to distinguish between the *on* and *off* states based on porphyrin fluorescence. The INHIBIT gate can be cycled a number of times, but gradually degrades after multiple switching, as was observed for the AND function.[41]

Other examples of molecular logic

The molecules discussed above illustrate the basic ideas underlying our approach to designing molecular switches and logic gates. We have used similar principles to design a number of other switches and gates. For example, dyad **6** (Fig. 13) consists of a photochromic nitrospiropyran moiety (Sp) covalently linked to a zinc (P_{Zn}) porphyrin.[42] The spiropyran (see **6a**), which absorbs only in the UV spectral region, may be photoisomerized using UV light to a mero-cyanine form (see **6b**) that absorbs strongly in the 600-nm region. The merocyanine readily reverts to the spiro form when irradiated with visible light, and also thermally closes to the spiro isomer. In **6**, as in the molecules discussed above, the photochrome controls the lifetime of the porphyrin first excited singlet state, and therefore the fluorescence quantum
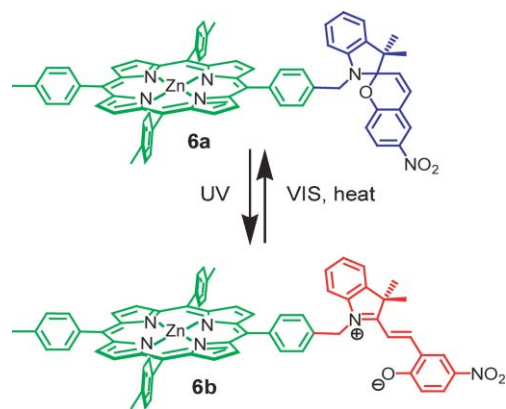
yield of the porphyrin. However, the control in this case is based on singlet–singlet energy transfer, rather than control of redox potentials. In **6a**, the porphyrin first excited singlet state is unperturbed by the closed form of the attached spiropyran, and fluoresces strongly. The lifetime of the porphyrin excited singlet state is 1.80 ns, which is typical for a zinc porphyrin of this type. Excitation of the spiropyran moiety in the 360-nm region results in ring opening to the merocyanine **6b**. The open form re-closes thermally in 2-methyltetrahydrofuran with a time constant of 20 s, or following irradiation into the 600 nm band. The lifetime of the zinc porphyrin excited state in **6b** is reduced to 130 ps by singlet–singlet energy transfer to the merocyanine moiety, leading to strong fluorescence quenching. The quantum yield of energy transfer is 0.93. This reversible photoswitchable quenching phenomenon provides light-activated control of the porphyrin excited state, and could be used to control subsequent energy or electron transfer processes that might be initiated by this excited state in more complex molecular photonic or optoelectronic devices. For example, we have reported a molecular switch consisting of a porphyrin bearing both a fullerene electron acceptor and a dithienylethene photochrome wherein the electron transfer from the porphyrin first excited singlet state to the fullerene is precluded by rapid singlet–singlet energy transfer to the closed form of the dithienylethene. No such energy transfer quench-ing is observed when the dithienylethene is in the open form, and efficient photoinduced electron transfer occurs.[43]

When photochromic molecular switches are designed to work in concert with suitable physical phenomena, even single photochromic chromophores may be used as logic gates. For example, like other dihydroindolizines, photochrome **7a** (Fig. 14) may be photoisomerized to its betaine form with UV light. Visible light or heat return **7b** to the spiro form. Although **7a** does not absorb light in the visible region, **7b**
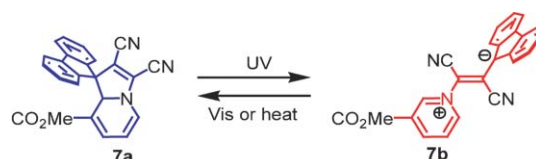

Fig. 14 Photochromic dihydroindolizine component of molecule-based AND gate based on electric linear dichroism.

absorbs strongly with a maximum at 585 nm. When a solution of **7b** is placed between two metal plates and a voltage is applied to these electrodes, a strong electric field (940 kV m^{-1}) is formed in the region of the molecules. Under these conditions, the visible transition of **7b** displays a strong electric linear dichroism (ELD). That is, the absorbance by the solution of light plane-polarized in the field direction increases in the presence of the field. This is because **7b** is a polar molecule, and therefore it partially orients along the electric field, partially aligning its transition moment with the plane of polarization. The ELD effect, coupled with the photochromic properties of **7**, allow the molecule to function as an AND gate.[44] The initial state of the gate is the spiro form **7a**. The two inputs are the electric field and UV light. The readout of the gate is the ELD effect. A strong ELD response signifies that the gate output is *on*. In the initial state, there is no ELD effect at 585 nm because **7a** does not absorb at this wavelength, and the electric field is not present. When the electric field (input A) is applied, no response is again obtained (because **7a** does not absorb at 585 nm, and is expected to have a relatively small dipole moment), and the gate is still *off*. If input B, UV light, is applied instead, **7a** isomerizes to **7b**. However, in the absence of an electric field, no ELD is observed, and the gate remains *off*. Finally, if both inputs are applied, **7a** is isomerized to **7b** and the electric field generates an ELD response. Thus, the requirements for an AND gate are fulfilled in an experimentally relatively simple apparatus.

A final example of molecule-based logic is a photonic Boolean half-adder that employs a solution of dyad **2** and triad **3** in 2-methyltetrahydrofuran.[25] Mathematical calculations require several gates operating together. The half-adder, a combination of an AND gate and an XOR (exclusive OR) gate that share two inputs, carries out binary addition. In combination, silicon-based half-adders perform the logic operations of modern computing. As shown in Table 3, each of the two inputs and outputs of a half-adder may be either *on* (designated 1) or *off* (0). As we have seen above, the AND gate gives an *on* response only when both inputs, A and B, are *on*. The XOR gate generates an *on* output when either input is *on*, but not when both inputs are *on*, or when both are *off*. In binary addition, the XOR gate output is the sum digit, and the AND gate output is the carry digit.

Fig. 15 shows the schematic diagram of the molecule-based half-adder. An optical cuvette contains a solution of molecules **2** and **3** which provide the XOR and AND gate functions, respectively. The photochemistry of each of these molecules was discussed above. When **3** is used in the photochemical AND gate, it is set initially in the CPD form. Irradiation of **3a** with light from either input laser A (1064 nm) or input laser B
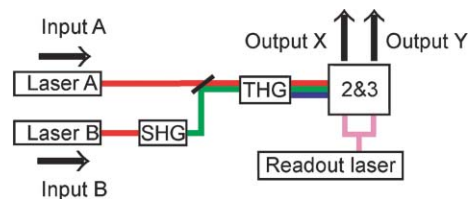

Fig. 15 Schematic diagram of the half adder. Molecules **2** and **3** in 2-methyltetrahydrofuran reside in a cuvette labeled "2 & 3". *Via* pulsed (5 ns pulses at 10 Hz for 10 min) Nd:YAG lasers, the cuvette may be irradiated at either 1064 nm (input A), or 532 nm *via* a second-harmonic generator (SHG, input B). When both inputs are on, the sample receives 355 nm irradiation from the third-harmonic generator crystal (THG). Outputs X (AND gate) and Y (XOR gate) are the long-lived transient absorbance of the fullerene radical anion and porphyrin fluorescence, respectively. The readout laser (650 nm) provides light for the porphyrin excitation needed to produce these outputs.

(532 nm) does not lead to photoisomerization, as the CPD moiety does not absorb at those wavelengths. Measurement of the transient absorbance at 1000 nm generated by a readout laser at 650 nm shows no $DHP^{\bullet+}-P-C_{60}^{\bullet-}$ (output X *off*). However, simultaneous irradiation by both lasers generates 355 nm light *via* the third-harmonic-generating crystal, and **3a** is switched to the DHP form, **3b**. Long-lived $C_{60}^{\bullet-}$ absorbance due to $DHP^{\bullet+}-P-C_{60}^{\bullet-}$ is detected *via* the readout laser system, and output X is turned *on*. Experimental observation of these logic operations within the half-adder is demonstrated in Fig. 16. After a logic operation, the state of the gate may be read out once or many times prior to resetting the gate to the $CPD-P-C_{60}$ state by irradiation at 532 nm.

When dyad **2** performs in the XOR gate, the molecule is set initially in the **2b** state with the photochrome in the betaine form. The readout of the gate (porphyrin fluorescence, output Y) is *off* because electron transfer quenches the porphyrin
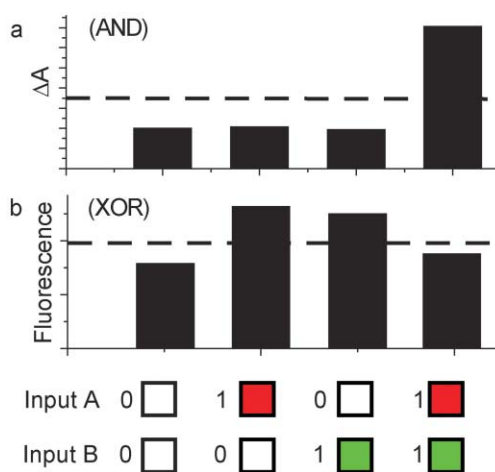
Table 3 Truth table for the half-adder

Input A	Input B	Output X AND gate (carry digit)	Output Y XOR gate (sum digit)	Binary sum
0	0	0	0	00
1	0	0	1	01
0	1	0	1	01
1	1	1	0	10

Fig. 16 (a) Experimental output (absorbance change at 1000 nm) for AND gate triad **3** after exposure to inputs at 1064 nm (red squares) and/or 532 nm (green squares). The dashed line is a threshold level for detection of an *on* response. (b) Experimental output (fluorescence at 720 nm) from XOR gate dyad **2** after exposure to the inputs. Note that the combination of outputs gives the half-adder function described in Table 3.

excited singlet state (see Fig. 16). Excitation at 1064 nm with input laser A thermally isomerizes **2b** to DHI form **2a**, electron transfer ceases, and the readout laser induces strong porphyrin fluorescence. Thus, output Y switches *on*. Similarly, irradiation of **2b** with input laser B at 532 nm leads to photoisomerization to **2a**, and fluorescence output Y is turned *on*. However, if both input lasers A and B are turned *on*, the 355 nm light produced by the THG does not induce net photoisomerization of **2b**. Electron transfer still occurs, and the fluorescence output Y remains *off*. The requirements for an XOR gate (Table 3) are met. After a logic operation, the gate may be reset to the P–BT state with 355 nm light.

The two molecular switches and the THG work together as a half-adder. The two shared inputs are laser beams at 1064 nm (input A) or 532 nm (input B). The output of the AND gate (output X, the carry digit) is the nanosecond transient absorbance of $DHP^{•+}–P–C_{60}^{•−}$ in **3b**. The output of the XOR gate (output Y, the sum digit) is the porphyrin fluorescence of $^1P–DHI$ in **2a**. (The porphyrin moiety in **3** is never significantly fluorescent.) Fig. 16 demonstrates the half-adder function experimentally. Initially, **3** is in the CPD–P–C_{60} form **3a**, and **2** is in the P–BT state **2b**. When both input beams are *off*, the outputs of both gates are also *off*. The output of the half-adder is the binary sum 00 (first row of Table 3). When input A is *on*, molecule **3** (AND) is not affected, but **2b** isomerizes to **2a**. The molecule fluoresces, switching the XOR output *on*. The output of the half-adder is 01 (1 in base-10). Alternatively, if input B at 532 nm is switched *on*, molecule **3a** is still not affected, and **2b** is again isomerized to P–DHI, leading to an *on* response for output Y. Again, the output of the half-adder is 01. Finally, if both inputs A and B are switched *on*, the 355 nm light from the THG converts **3a** to **3b**, and long-lived charge separation leads to an *on* response from output X (carry digit). Because the population of **2b** is not significantly affected by the 355 nm light, the XOR output remains *off*. The corresponding output of the half-adder is the binary sum 10 (2 in base-10), completing the truth table.

After readout, the half-adder is reset to the initial state using 355 nm (**2**) and 532 nm (**3**) light. The quantum yield of isomerization at 532 nm is about 50 times higher for **3** than for **2**, permitting the AND gate to be reset by the 532 nm light without significantly affecting the XOR gate. The results of photochemical cycling of **3** and **2** in the AND gate configuration were investigated. Although triad **3** is unchanged after 8 cycles, **2** undergoes some decomposition.

Note that the THG, which is integral to the gate operation, provides a transient signal that is only present during the laser pulses. It affects **2** and **3** differently, which allows it to contribute to the functions of both gates. The photochromes of **2** and **3** are molecular switches that record the results of the transient inputs for interrogation at a convenient later time, after the inputs have been turned off. The remaining parts of **2** and **3** provide the readouts, which must be different for the two gates.

Each state of the half-adder has a lifetime of $\geqslant 1$ h at ambient temperatures. The photochemical events leading to the readouts for **2** and **3** have time constants $\leqslant 2$ μs. The pulsed laser inputs A and B are applied for $\leqslant 10$ min, but the total irradiation time is actually $\leqslant 30$ μs per input. Thus, the half-adder is capable of relatively rapid cycle times if light intensity is sufficient.

Although the current device is not suitable for the construction of useful computers, it points the way to possible applications. The inputs and outputs are all optical, and no diffusional processes or bimolecular chemical reactions are required. Thus, this approach to molecule-based logic is suitable for non-fluid media, and the inputs and outputs do not require physical access, except by light. After receiving inputs, the half-adder remains latched in the resulting state for hours, facilitating single or multiple readouts, and can then be reset with light. The device is capable of cycle times on the order of tens of microseconds or less. Although half-adder function has been demonstrated here with optical outputs, both outputs are based on intramolecular electron transfer reactions, and in principle could be detected electronically if the molecules were suitably "wired" into circuits.

Conclusions

As illustrated by the molecules discussed above, basic photochemical processes, such as singlet–singlet energy transfer, photoinduced electron transfer, and photoisomerization, may be used in the design of synthetic molecules that act as photochemically-controlled switches and logic gates. The outputs of such gates may be optical (*e.g.*, fluorescence or transient absorbance), but in principle, they could be electrical in situations where electron transfer is switched on or off. In these cases, it would be useful to "wire" molecules into electronic circuits so that the response could be read out *via* conventional means. However, incorporating such molecules into circuits is thus far not practical. Practical application of these ideas would also raise questions concerning the long-term stability of the organic molecules during irradiation and under environmental operating conditions for the intended use. Molecule-based, optically controlled logic systems offer potential advantages because the switching and readout operations require no physical access other than by light. They could in principle be "multiplexed" by mixing of several types of gate, addressable with different wavelengths, in the same volume element, and three-dimensional arrays of elements could be envisioned. Our goal in this work has not been to develop practical applications, but rather to devise photochemical strategies for achieving the various switching effects and to design molecular systems in which these strategies can be implemented. Progress in this area will require not only developing molecules capable of additional logic operations and ensuring their suitability for a given device, but also devising methods for communication of information between the molecular switches.

Acknowledgements

References

1 D. Kuciauskas, S. Lin, G. R. Seely, A. L. Moore, T. A. Moore, D. Gust, T. Drovetskaya, C. A. Reed and P. D. W. Boyd, *J. Phys. Chem.*, 1996, **100**, 15926.
2 *Organic Photochromic and Thermochromic Compounds*, ed. J. C. Crano and R. J. Guglielmetti, Plenum Press, New York, 1998.
3 A. Aviram, *J. Am. Chem. Soc.*, 1988, **110**, 5687.
4 V. Balzani, A. Credi and M. Venturi, *ChemPhysChem*, 2003, **3**, 49.
5 A. P. de Silva, D. B. Fox, T. S. Moody and S. M. Weir, *Pure Appl. Chem.*, 2001, **73**, 503.
6 P. Ball, *Nature*, 2000, **406**, 118.
7 D. Kuciauskas, P. A. Liddell, A. L. Moore, T. A. Moore and D. Gust, *J. Am. Chem. Soc.*, 1998, **120**, 10880.
8 F. Pina, M. J. Melo, M. Maestri, P. Passaniti and V. Balzani, *J. Am. Chem. Soc.*, 2000, **122**, 4496.
9 A. Credi, V. Balzani, S. J. Langford and J. F. Stoddart, *J. Am. Chem. Soc.*, 1997, **119**, 2679.
10 S. J. Langford and T. Yann, *J. Am. Chem. Soc.*, 2003, **125**, 11198.
11 T. Gunnlaugsson, D. A. Mac Donaill and D. Parker, *J. Am. Chem. Soc.*, 2001, **123**, 12866.
12 A. P. de Silva, I. M. Dixon, H. Q. N. Gunaratne, T. Gunnlaugsson, P. R. S. Maxwell and T. E. Rice, *J. Am. Chem. Soc.*, 1999, **121**, 1393.
13 P. Ghosh and P. K. Bharadwaj, *J. Am. Chem. Soc.*, 1996, **118**, 1553.
14 A. P. de Silva and N. D. McClenaghan, *Chem. Eur. J.*, 2002, **8**, 4935.
15 H. Xu, X. Xu, R. Dabestani, G. M. Brown, L. Fan, S. Patton and H. F. Ji, *J. Chem. Soc., Perkin Trans. 2*, 2002, 636.
16 F. M. Raymo and S. Giordani, *J. Am. Chem. Soc.*, 2002, **124**, 2004.
17 F. M. Raymo and S. Giordani, *Proc. Natl. Acad. Sci. USA*, 2002, **99**, 4941.
18 A. Saghatelian, N. H. Volcker, K. M. Guckian, V. S. Y. Lin and M. R. Ghadiri, *J. Am. Chem. Soc.*, 2003, **125**, 346.
19 K. L. Kompa and R. D. Levine, *Proc. Natl. Acad. Sci. USA*, 2001, **98**, 410.
20 A. P. de Silva and N. D. McClenaghan, *J. Am. Chem. Soc.*, 2000, **122**, 3965.
21 M. N. Stojanovic and D. Stefanovic, *J. Am. Chem. Soc.*, 2003, **125**, 6673.
22 M. N. Stojanovic, T. E. Mitchell and D. Stefanovic, *J. Am. Chem. Soc.*, 2002, **124**, 3555.
23 X. Guo, D. Zhang, G. Zhang and D. Zhu, *J. Phys. Chem. B*, 2004, **108**, 11942.
24 X. Guo, D. Zhang, H. Tao and D. Zhu, *Org. Lett.*, 2004, **6**, 2491.
25 J. Andréasson, G. Kodis, Y. Terazono, P. A. Liddell, S. Bandyopadhyay, R. H. Mitchell, T. A. Moore, A. L. Moore and D. Gust, *J. Am. Chem. Soc.*, 2004, **126**, 15926.
26 Y. Terazono, G. Kodis, J. Andréasson, G. Jeong, A. Brune, T. Hartmann, H. Dürr, A. L. Moore, T. A. Moore and D. Gust, *J. Phys. Chem. B*, 2004, **108**, 1812.
27 H. Dürr and H. Bouas-Laurent, *Photochromism: Molecules and Systems*, Elsevier, Amsterdam, 1990.
28 H. Dürr, *Organic Photochromic and Thermochromic Compounds*, ed. J. C. Crano and R. J. Guglielmetti, Plenum Press, New York, 1999, **1**, p. 223.
29 P. A. Liddell, G. Kodis, J. Andréasson, L. de la Garza, S. Bandyopadhyay, R. H. Mitchell, T. A. Moore, A. L. Moore and D. Gust, *J. Am. Chem. Soc.*, 2004, **126**, 4803.
30 R. H. Mitchell, *Eur. J. Org. Chem.*, 1999, **1999**, 2695.
31 R. H. Mitchell, T. R. Ward, Y. Wang and P. W. Dibble, *J. Am. Chem. Soc.*, 1999, **121**, 2601.
32 M. A. L. Sheepwash, T. R. Ward, Y. Wang, S. Bandyopadhyay, R. H. Mitchell and C. Bohne, *Photochem. Photobiol. Sci.*, 2003, **2**, 104.
33 D. Gust and T. A. Moore, *The Photosynthetic Reaction Center*, ed. J. R. Norris and J. Deisenhofer, Academic Press, New York, 1993, p. 419.
34 D. Gust, T. A. Moore and A. L. Moore, *J. Photochem. Photobiol., B*, 2000, **58**, 63.
35 D. Gust, T. A. Moore and A. L. Moore, *Acc. Chem. Res.*, 2001, **34**, 40.
36 S. D. Straight, J. Andréasson, G. Kodis, A. L. Moore, T. A. Moore and D. Gust, *J. Am. Chem. Soc.*, 2005, **127**, 2717.
37 R. A. Marcus, *J. Chem. Phys.*, 1956, **24**, 966.
38 R. A. Marcus and N. Sutin, *Biochim. Biophys. Acta*, 1985, **811**, 265.
39 N. S. Hush, *Trans. Faraday Soc.*, 1961, **57**, 557.
40 N. S. Hush, *J. Chem. Phys.*, 1958, **28**, 962.
41 S. D. Straight, J. Andréasson, G. Kodis, S. Bandyopadhyay, R. H. Mitchell, T. A. Moore, A. L. Moore and D. Gust, *J. Am. Chem. Soc.*, 2005, **127**, 9403.
42 J. L. Bahr, G. Kodis, L. de la Garza, S. Lin, A. L. Moore, T. A. Moore and D. Gust, *J. Am. Chem. Soc.*, 2001, **123**, 7124.
43 P. A. Liddell, G. Kodis, A. L. Moore, T. A. Moore and D. Gust, *J. Am. Chem. Soc.*, 2002, **124**, 7668.
44 J. Andréasson, Y. Terazono, B. Albinsson, T. A. Moore, A. L. Moore and D. Gust, *Angew. Chem., Int. Ed.*, 2005, **44**, 7591.